Available online at www.sciencedirect.com
ScienceDirect
Bioorganic & Medicinal Chemistry Letters 17 (2007) 5783–5789
Bioorganic & Medicinal Chemistry Letters

N^4-Phenyl modifications of N^2-(2-hydroxyl)ethyl-6-(pyrrolidin-1-yl)-1,3,5-triazine-2,4-diamines enhance glucocerebrosidase inhibition by small molecules with potential as chemical chaperones for Gaucher disease

Wenwei Huang,[a] Wei Zheng,[a] Daniel J. Urban,[b] James Inglese,[a] Ellen Sidransky,[b,*] Christopher P. Austin[a] and Craig J. Thomas[a,*]

[a]*NIH Chemical Genomics Center, National Human Genome Research Institute, NIH, 9800 Medical Center Drive, MSC 3370, Bethesda, MD 20892-3370, USA*
[b]*Medical Genetics Branch, National Human Genome Research Institute, NIH, Bld 35 Rm1A213, 35 Convent Drive, Bethesda, MD 20892-3708, USA*

Received 3 August 2007; revised 23 August 2007; accepted 23 August 2007
Available online 28 August 2007

Abstract—A series of 1,3,5-triazine-2,4,6-triamines were prepared and analyzed as inhibitors of glucocerebrosidase. Synthesis, structure activity relationships and the selectivity of chosen analogues against related sugar hydrolases enzymes are described.
Published by Elsevier Ltd.

Glycosphingolipids are cell membrane components that maintain the stability of the lipid bilayer, function as cellular recognition elements and play an important role in cellular adherence.[1] These important cellular constructs are comprised of varying polysaccharide chains linked to ceramide via a glycosidic bond. Glycosphingolipids are ultimately targeted for degradation through the action of selected lysosomal hydrolases.[2] Several different diseases arise when a defect in one or more of these hydrolases causes non-degraded glycosphingolipids to accumulate within the lysosome.[3] These maladies are commonly referred to as 'lysosomal storage disorders' and include Niemann-Pick, Tay–Sachs and Gaucher diseases.

Gaucher disease results from mutations in the glucocerebrosidase (GC) gene. Many of these are point mutations that result in a misfolded protein with diminished catalytic activity or aberrant trafficking from the endoplasmic reticulum to the lysosome.[2,3] Over 200 different mutations giving rise to Gaucher disease have been identified, and it is likely that multiple misfolded protein conformations exist.[4] Current treatment for Gaucher disease involves enzyme replacement therapy.[5] While this therapy alleviates many of the systemic manifestations of the disease, including hepatosplenomegaly, anemia and thrombocytopenia, the inability of recombinant enzyme to cross the blood–brain barrier prevents amelioration of the CNS associated symptoms in neuronopathic forms of Gaucher disease. The subset of mutations that result in protein misfolding and improper trafficking of GC to the lysosome presents an opportunity for the use of 'chemical chaperone' therapy, and importantly, could provide a therapeutic approach capable of penetrating the blood–brain barrier.

Chemical chaperones are small molecules that bind to misfolded proteins, restoring correct structural conformation and enabling appropriate protein trafficking.[6] Once the chaperoned protein reaches its appropriate subcellular location, the small molecule chaperone must either be displaced by native substrate to allow for the continued presence of a correctly folded, active protein, or bind to an allosteric site that does not disrupt substrate binding. The utility of chaperone therapy in Gaucher, Sandhoff, Fabry and Tay–Sachs diseases has been studied.[7,8] Kelly and coworkers,[9] Overkleeft and coworkers[10] and Fan and

Keywords: Triazine; Gaucher disease; Glucocerebrosidase; Chemical chaperone.
* Corresponding authors. Tel.: +1 301 217 4079; fax: +1 301 217 5736 (C.J.T.); tel.: +1 301 451 0901, +1 301 496 0373; fax: +1 301 402 6438 (E.S.); e-mail addresses: sidranse@mail.nih.gov; craigt@mail.nih.gov

0960-894X/$ - see front matter Published by Elsevier Ltd.
doi:10.1016/j.bmcl.2007.08.050

coworkers[11] have advanced several iminosugars designed to mimic the native glycosphingolipid substrate as potential GC chaperones. Several of these small molecules are currently being evaluated in clinical trials.[8] In addition, at least one reported non-sugar based small molecule (1-phenyl-2-decanoylamino-3-morpholino-1-propanol), which was designed as a ceramide mimic, is also being studied clinically.[8] We recently reported the use of qHTS to identify three novel, structurally distinct small molecule inhibitors of GC including 2-(4-(5-chloro-2-methoxyphenylamino)-6-(pyrrolidin-1-yl)-1,3,5-triazin-2-ylamino)ethanol (**1**), *N*-(4-methyl-2-morpholinoquinolin-6-yl)cyclohexanecarboxamide (**2**) and *N*-(5-ethyl-1,3,4-thiadiazol-2-yl)-4-(phenylsulfonamido)benzamide (**3**) (Fig. 1).[12] These novel GC inhibitors possess potencies comparable to the best iminosugars, including the clinically relevant *N*-butyl-deoxynojirimycin (Miglustat) (**4**) [for **1**: IC_{50} = 0.70 μM; for **2**: IC_{50} = 0.031 μM; for **3**: IC_{50} = 0.070 μM]. A significant property of these structures is their apparent selectivity versus related sugar hydrolases including α-glucosidase, α-galactosidase and β-hexosaminidase.

It has been demonstrated that the ability of iminosugars to act as chemical chaperones is dependent upon the nature of the specific mutant protein.[13] Further, Kelly and coworkers have shown that temperature alterations have differential effects on the cellular trafficking of selected GC variants.[14] These studies suggest that differing mutant forms of GC likely result in distinctive protein misfolding. Taken together with the vast number of clinically relevant GC mutations, these findings emphasize the value of developing divergent small molecule chemotypes to target alternate folded proteins.

Previously, we evaluated the ability of these novel GC inhibitors to act as chemical chaperones and found that the least potent structural series (the 1,3,5-triazine-2,4,6-triamine core represented by **1**) possessed the greatest chaperone activity.[12] This intriguing finding prompted us to further explore and optimize this series of compounds. To this end, we synthesized and evaluated numerous analogues of **1** by examining three discrete sections of the compounds; the aminoethanol moiety, the pyrrolidinyl moiety and the substituted aniline moiety.

The synthetic methods for the construction of substituted triazines are well documented.[15] We utilized a three step, one pot procedure (Scheme 1) whereby cyanuric chloride is treated first with substituted aniline (see Table 3) in acetonitrile with (method B) or without (method A) Hunig's base.[16] Following this transformation, primary or secondary amines (see Table 2) were administered in either 3.3 equiv (method A) or 1.1 equiv (method B) in DMA with Hunig's base for 10 min. Finally, a large excess of primary and secondary alkyl and cycloalkylamines (see Table 1) was added and stirred for 4–8 h and the resulting mixture was purified via mass-directed preparative HPLC. Yields for the one pot, three step procedure were typically in excess of 60%. Each construct was examined by LCMS and ELSD for purity and characterized via ^{1}H NMR, high-resolution mass spectrometry and ^{13}C NMR for selected analogues.[17] Individual compounds were evaluated biochemically[18] from standard 10 μM DMSO solutions via a GC enzyme assay utilizing a fluorogenic resorufin β-D-glucopyranoside substrate as previously reported.[12]

Our first investigations addressed the SAR of the ethanolamine moiety (Table 1). The qHTS screen revealed **1** as a potent inhibitor of GC from a collection of nearly 400 related triazine structures that did not maintain an ethanolamine moiety. As anticipated, our subsequent attempts to modify this substructure were collectively detrimental. It was also noted that deviations from any substructure that did not contain a hydroxyl group

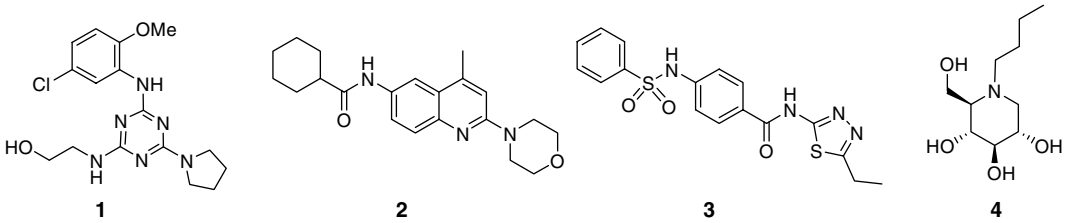

Figure 1. Compound structures of previously reported inhibitors of glucocerebrosidase including 2-(4-(5-chloro-2-methoxyphenylamino)-6-(pyrrolidin-1-yl)-1,3,5-triazin-2-ylamino)ethanol (**1**), *N*-(4-methyl-2-morpholinoquinolin-6-yl)cyclohexanecarboxamide (**2**) and *N*-(5-ethyl-1,3,4-thiadiazol-2-yl)-4-(phenylsulfonamido)benzamide (**3**) and *N*-butyl-deoxynojirimycin (Miglustat) (**4**).

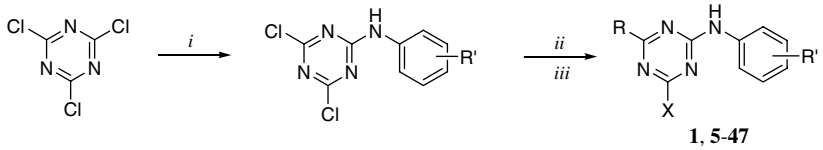

Scheme 1. Reagents and conditions: Method A. (i) Substituted ArNH2 (1 equiv), ACN, rt 4 h; (ii) substituted amine (3.3 equiv), Hunig's base, DMA, rt 10 min; (iii) substituted amine (5–10 equiv), rt 4–8 h. Method B. (i) Substituted ArNH2 (1 equiv), Hunig's base, ACN, rt 4 h; (ii) substituted amine (1.05 equiv), Hunig's base, DMA, rt 10 min; (iii) substituted amine (5–10 equiv), rt 4–8 h.

Table 1. SAR surrounding the ethanolamine moiety of the core triazine scaffold

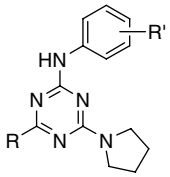

Analogue #	R	R′	GC inhibition IC_{50} (μM) and SD[a]
1	$-NHCH_2CH_2OH$	2-OMe, 5-Cl	0.70 ± 0.08
5	$-NHCH_2CH_2OCH_3$	2-OMe, 5-Cl	Inactive
6	$-N(CH_2CH_2OH)_2$	2-OMe, 5-Cl	Inactive
7	$-NHCH_2CH_2CH_2CH_3$	2-OMe, 5-Cl	7.77 ± 0.33
8	$-NHCH_2Ph$	2-OMe, 5-Cl	Inactive
9	$-NHCH_2$(2-furanyl)	2-OMe, 5-Cl	Inactive
10	$-NH_2$	2-OMe, 5-Cl	Inactive
11	$-NHCH_2CH_2NHCOCH_3$	2-OMe	Inactive
12	$-NHCH_2CH(OH)CH_3$	2-OMe	20.70
13	$-NHCH_2CH(OH)CH_2Ph$	2-OMe	6.80 ± 0.83
14	$-NHCH_2CONH_2$	2-OMe	Inactive
15	$-NHCH_2CH_2CH_2CH_2OH$	2-OMe	Inactive
16	$-NHCH_2COOMe$	2-OMe	Inactive

[a] Error represents the standard deviation determined from three separate experiments.

Table 2. SAR surrounding the pyrrolidine moiety of the core triazine scaffold

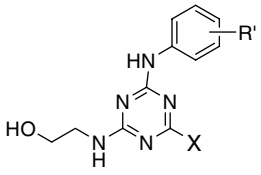

Analogue #	X	R′	GC inhibition IC_{50} (μM) and SD[a]
1	Pyrrolidin-1-yl	2-OMe, 5-Cl	0.70 ± 0.08
17	Morpholin-1-yl	2-OMe, 5-Cl	12.13
18	*N*,*N*-Diethylamino	2-OMe, 5-Cl	Inactive
19	Piperidin-1-yl	2-OMe, 5-Cl	31.10
20	Azepan-1-yl	2-OMe, 5-Cl	Inactive
21	*N*-(*n*-Butyl)amino	2-OMe	6.1 ± 0.51
22	*N*-Benzylamino	2-OMe	18.80
23	3,3-Difluoropyrrolidin-1-yl	2-OMe	7.75 ± 0.82
24	Azetidin-1-yl	2-OMe	2.31 ± 0.28

[a] Error represents the standard deviation determined from three separate experiments.

conferred difficulty with water solubility. This observation is supported by the calculated *c*Log *P* values of selected analogues as illustrated by the comparison of **1** (calculated *c*Log *P* of 3.35) with **7** (calculated *c*Log *P* of 5.23). Additional compounds were made and examined including the 2-aminoethyl analogue and showed no apparent activity (data are not shown due to insufficient purity analysis—typically less than 80% pure by HPLC UV/vis peak integration).

We next attempted to optimize the inhibitory potential of this series through alterations at the pyrrolidinyl moiety (Table 2). Here again, deviations from this core component were found to be adverse in terms of GC inhibition. Interestingly, altering a pyrrolidinyl to a *N*,*N*-diethylamino moiety (analogue **18**) that maintained the same relative size, yet lost the rigid ring structure, resulted in an analogue that was completely inactive. Rings of a larger size (6 and more) were significantly less potent and the only smaller ring system explored (the 4-membered azetidinyl ring) was modestly potent, yet significantly less than the core pyrrolidinyl moiety found in **1** and **31**.

Finally, optimizations of the anilinyl moiety were examined (Table 3). Within this substructure we first focused on the existing 2-methoxy, 5-chloro substitution pattern by exploring selected replacements and deletions in terms of mono- versus di-substitution and relative position (ortho, meta and para). While the majority of these analogues (for example **28**–**30**, **31**–**34**) remained modestly potent, none surpassed the original ligand. We also

Table 3. SAR surrounding the aniline moiety of the core triazine scaffold

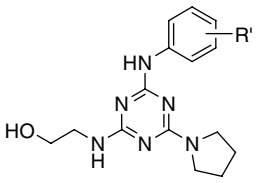

Analogue #	R′	GC inhibition IC_{50} (μM) and SD[a]
1	2-OMe, 5-Cl	0.70 ± 0.80
25	2-Me	3.94 ± 0.13
26	3-Me	6.19 ± 0.46
27	4-Me	10.04
28	2-Cl	28.97
29	3-Cl	6.69 ± 0.27
30	4-Cl	6.34 ± 0.06
31	2-OMe	1.08 ± 0.13
32	3-OMe	8.25 ± 0.21
33	4-OMe	8.80 ± 0.64
34	2-OH	2.00 ± 0.14
35	2-OEt	0.77 ± 0.04
36	2-OPh	21.67
37	2-O*t*-Bu	0.33 ± 0.06
38	2-OBn	31.4
39	2-OCF_3	3.34 ± 0.06
40	2-SMe	2.39 ± 0.09
41	2-OMe, 5-OMe	1.53 ± 0.08
42	2-OMe, 4-OMe	4.90 ± 0.13
43	2-OMe, 5-CF_3	2.65 ± 0.14
44	2-OMe, 5-Ph	2.22 ± 0.04
45	2-NO_2	Inactive
46	2-$CONH_2$	Inactive
47	2-$NHCOCH_3$	Inactive
48	2-OH, 5-Cl	0.73 ± 0.09
49	2-OH, 5-Ph	0.37 ± 0.05
50	2-OEt, 5-Cl	0.96 ± 0.02
51	2-O*i*-Pr, 5-Cl	3.44 ± 0.08
52	2-O*t*-Bu, 5-Cl	1.04 ± 0.05
53	H	16.47

[a] Error represents the standard deviation determined from three separate experiments.

explored various commonly applied substitutions including methyl (analogues **25**–**27**) di-methoxy (analogues **41**, **42**) and trifluoromethoxy (analogue **39**) with limited success. We next investigated the consequence of altering a 2-OMe group (analogue **31**) to a 2-OEt group (analogue **35**). This change resulted in a modest potency enhancement relative to the mono-substituted 2-OMe analogue. We further evaluated this trend by expanding this moiety into a 2-OPh (analogue **36**) and 2-O*t*-Bu (analogue **37**). Gratifyingly, **37** provided an IC_{50} value of 0.33 μM, the lowest reported potency for this structural class of GC inhibitors. Unfortunately, this SAR was not found to be enhanced by incorporation of the previously noted disubstituted analogues containing a 5-Cl substitution in conjugation with the 2-alkoxy series (analogues **50**–**52**). Continued explorations also revealed that a 2-OH, 5-Ph substitution (analogue **49**) conferred an IC_{50} value of 0.37 μM. Thus, the two most potent analogues possessed structurally unrelated substitution patterns and only modestly related calculated *c*Log *P* values (calculated *c*Log *P* of 3.72 for **37** and calculated *c*Log *P* of 4.22 for **49**). Efforts to ascertain the binding site through co-crystallization and docking studies will be pursued.

Having found novel analogues with improved potency, it was important to confirm that they maintained the selectivity profile of the parent compound (**1**) versus the related hydrolases α-glucosidase, α-galactosidase and β-hexosaminidase.[18] Importantly, **37** showed no activity against any of these related enzymes at concentrations up to 77 μM (Fig. 2).

Through manipulations of the N^4-phenyl moiety, we optimized the inhibitory activity of a small molecule shown to possess strong chemical chaperone activity and arrived at novel analogue **37** with an IC_{50} value of 330 nM. The expanded compound set provides numerous analogues with GC enzyme inhibitory potencies ranging from 0.3 μM to 2.0 μM. This family of inhibitors, as well as those from ongoing studies based upon **2** and **3**, will enable us to probe the relationship between enzymatic inhibitory potency and chaperone activity. Expanded compound sets of divergent structures that maintain a range of potencies may represent crucial probe compounds that will permit further characterization of various GC mutants. Moreover, since different mutant forms of GC are likely to require different chemical chaperones, these expanded compound sets will facilitate exploration of the potential for mutation-specific chemical chaperones.

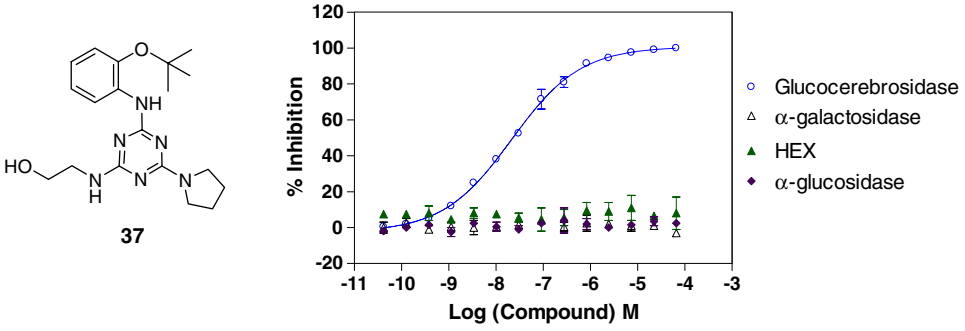

Figure 2. Selective inhibition of glucocerebrosidase (◇), α-glucosidase (♦), α-galactosidase (Δ) and β-hexosaminidase (▲) by **37**. Data represent the collective results of three independent experiments performed in triplicate.

Acknowledgments

The authors thank Jeremy Smith, Adam Yasgar and Paul Shinn for assistance in compound management. The authors thank Bryan Mott and Mary E. LaMarca for helpful discussion and critical reading of this manuscript. Thanks also to Bev Chamberlin at MSU Mass Spectrometry Facility for HRMS analyses. This research was supported by the Molecular Libraries Initiative of the National Institutes of Health Roadmap for Medical Research and the Intramural Research Program of the National Human Genome Research Institute, National Institutes of Health.

References and notes

1. Wedeking, A.; van Echten-Deckert, G. *Curr. Org. Chem.* **2007**, *11*, 579.
2. Sawkar, A. R.; D'Haeze, W.; Kelly, J. W. *Cell. Mol. Life Sci.* **2006**, *63*, 1179.
3. Futerman, A. H.; van Meer, G. *Nat. Rev. Mol. Cell Biol.* **2004**, *5*, 554.
4. Hruska, K. S.; LaMarca, M. E.; Sidransky, E. In *Gaucher Disease*; Futerman, A. H., Zimran, A., Eds.; CRC Press: Boca Raton, FL, 2006; p 13.
5. Barton, N. W.; Brady, R. O.; Dambrosia, J. M.; Dibisceglie, A. M.; Doppelt, S. H.; Hill, S. C.; Mankin, H. J.; Murray, G. J.; Parker, R. I.; Argoff, C. E., et al. *N. Engl. J. Med* **1991**, *324*, 1464.
6. Sawker, A. R.; Cheng, W.-C.; Beutler, W.; Wong, C.-H.; Balch, W. E.; Kelly, J. W. *Proc. Natl. Acad. Sci. U.S.A.* **2002**, *99*, 15428.
7. Fan, J.-Q. *Trends Pharmacol. Sci.* **2003**, *24*, 355.
8. Butters, T. D. *Expert Opin. Pharmacother.* **2007**, *8*, 427.
9. Yu, Z.; Sawker, A. R.; Whalen, L. J.; Wong, C.-H.; Kelly, J. W. *J. Med. Chem.* **2007**, *50*, 94.
10. Wennekes, T.; van der Berg, R. J. B. H. N.; Donker, W.; van der Marel, G. A.; Strijland, A.; Aerts, J. M. F. G.; Overkleeft, H. S. *J. Org. Chem.* **2007**, *72*, 1088.
11. Zhu, X.; Sheth, K. A.; Li, S.; Chang, H.-H.; Fan, J.-Q. *Angew. Chem. Int. Ed.* **2005**, *44*, 7450.
12. Zheng, W.; Padia, J.; Urban, D. J.; Jadhav, A.; Goker-Alpan, O.; Simeonov, A.; Goldin, E.; Auld, D.; LaMarca, M. E.; Inglese, J.; Austin, C. P.; Sidransky, E. *Proc. Natl. Acad. Sci. U.S.A.* **2007**, *104*, 13192.
13. Sawker, A. R.; Adamski-Werner, S. L.; Cheng, W.-C.; Wong, C.-H.; Beutler, E.; Zimmer, K.-P.; Kelly, J. W. *Chem. Biol.* **2005**, *12*, 1235.
14. Sawker, A. R.; Schmitz, M.; Zimmer, K.-P.; Reczek, D.; Edmunds, T.; Balch, W. E.; Kelly, J. W. *ACS Chem. Biol.* **2006**, *1*, 235.
15. Katiyar, S. B.; Srivastava, K.; Puri, S. K.; Chauhan, P. M. S. *Bioorg. Med. Chem. Lett.* **2005**, *15*, 4957.
16. The majority of substituted anilines were commercially available. However 5-chloro-2-ethoxyaniline, 5-chloro-2-isopropoxyaniline, 2-*tert*-butoxyaniline and 2-*tert*-butoxy-5-chloroaniline required independent syntheses. The method was modified from a procedure by Wandless and coworkers (Woiwode, T. F.; Rose, C.; Wandless, T. J. *J. Org. Chem.* **1998**, *63*, 9594). Substituted anilines were utilized directly following a purifying extraction.

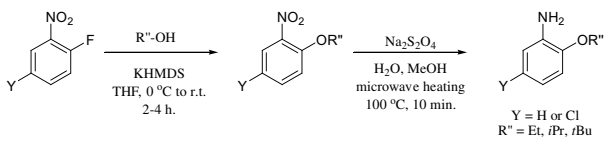

17. Spectroscopic data for **1**, **5**–**53** [Note: Several peaks within the proton and carbon NMR spectrum existed as rotomers that coalesce upon heating to 60 °C. This is a well-established phenomenon associated with triazine scaffolds (see Arvanitis et al. *J. Med. Chem.* **1999**, *42*, 805; Hajduk et al. *J. Med. Chem.* **1999**, *42*, 3852 and Leftheris et al. *J. Med. Chem.* **2004**, *47*, 6283 for examples)]: **1** ^{1}H NMR (400 MHz, DMSO-d_6) δ 8.64 (d, 1H, J = 6.6 Hz), 7.37–7.28 (m, 1H), 7.05–6.94 (m, 3H), 4.74–4.66 (m, 1H), 3.90 (s, 3H), 3.60–3.33 (m, 8H), 1.92 (br s, 4H); HRMS (ESI): *m/z* calcd for $C_{16}H_{21}ClN_6O_2$ $[M+1]^+$ 365.1493, found 365.1492. **5** ^{1}H NMR (400 MHz, DMSO-d_6) δ 8.63 (d, 1H, J = 2.3 Hz), 7.39–7.28 (m, 1H), 7.05–6.98 (m, 3H), 3.91 (s, 3H), 3.51–3.30 (m, 11H), 1.91 (br s, 4H); HRMS (ESI): *m/z* calcd for $C_{17}H_{23}ClN_6O_2$ $[M+1]^+$ 379.1649, found 379.1644. **6** ^{1}H NMR (400 MHz, DMSO-d_6) δ 8.60 (d, 1H, J = 2.3 Hz), 7.36 (s, 1H), 7.05 (d, 1H, J = 8.8 Hz), 6.99 (dd, 1H, J = 8.6, 2.5 Hz), 4.80–4.77 (m, 2H), 3.91 (s, 3H), 3.66 (br s, 8H), 3.56–3.46 (m, 4H), 1.93 (br s, 4H); HRMS (ESI): *m/z* calcd for $C_{18}H_{25}ClN_6O_3$ $[M+1]^+$ 409.1755, found 409.1766. **7** ^{1}H NMR (400 MHz, DMSO-d_6) δ 8.68–8.62 (m, 1H), 7.35–7.24 (m, 1H), 7.16–6.97 (m, 3H), 3.91 (s, 3H), 3.51–3.27 (s, 6H), 1.91 (br s, 4H), 1.57–1.50 (m, 2H), 1.42–1.32 (m, 2H), 0.93 (t, 3H, J = 7.4 Hz); HRMS (ESI): *m/z* calcd for $C_{18}H_{25}ClN_6O$ $[M+1]^+$ 377.1857, found 377.1860. **8** ^{1}H NMR (400 MHz, DMSO-d_6) δ 8.62–8.56 (m, 1H), 7.74–7.62 (m, 1H), 7.39–7.20 (m, 6H), 7.04–6.97 (m, 2H), 4.51–4.49 (m, 2H), 3.90 (br s, 3H), 3.49–3.27 (m, 4H), 1.92 (s, 4H); HRMS (ESI): *m/z* calcd for $C_{21}H_{23}ClN_6O$ $[M+1]^+$ 411.1700, found 411.1709. **9** ^{1}H NMR (400 MHz, DMSO-d_6) δ 8.63 (d, 1H, d = 2.5 Hz), 7.38–7.28 (m, 1H), 7.05–6.97 (m, 3H), 4.06–3.98 (m, 1H), 3.90 (s, 3H), 3.82–3.28 (m, 8H), 1.96–1.78 (m, 7H), 1.68–1.58 (m, 1H); HRMS (ESI): *m/z* calcd for $C_{19}H_{25}ClN_6O_2$ $[M+1]^+$ 405.1806, found 405.1800. **10** ^{1}H NMR (400 MHz, DMSO-d_6) δ 8.62 (d, 1H, J = 2.5 Hz), 7.30 (s, 1H), 7.05–6.97 (m, 2H), 6.59 (br s, 2H), 3.90 (s, 3H), 3.52–3.38 (m, 4H), 1.92 (br s, 4H); HRMS (ESI): *m/z* calcd for $C_{14}H_{17}ClN_6O$ $[M+1]^+$ 321.1231, found 321.1237. **11** ^{1}H NMR (400 MHz, DMSO-d_6) δ 8.47–8.44 (m, 1H), 7.96–7.90 (m, 1H), 7.35–7.26 (m, 1H), 7.04–6.93 (m, 4H), 3.90 (s, 3H), 3.51–3.22 (m, 8H), 1.91 (br s, 4H), 1.83 (s, 3H); HRMS (ESI): *m/z* calcd for $C_{18}H_{25}N_7O_2$ $[M+1]^+$ 372.2148, found 372.2147. **12** ^{1}H NMR (400 MHz, DMSO-d_6) δ 8.46 (d, 1H, J = 7.2 Hz), 7.33–7.26 (m, 1H), 7.05–6.80 (m, 4H), 4.84–4.68 (m, 1H), 3.90 (br s, 3H), 3.89–3.68 (m, 1H), 3.60–3.17 (m, 6H), 1.91 (br s, 4H), 1.09 (d, 3H, J = 6.3 Hz); HRMS (ESI): *m/z* calcd for $C_{17}H_{24}N_6O_2$ $[M+1]^+$ 345.2039, found 345.2041. **13** ^{1}H NMR (400 MHz, DMSO-d_6) δ 8.48–8.39 (m, 1H), 7.39–7.24 (m, 6H), 7.08–6.80 (m, 4H), 5.63–5.44 (m, 1H), 4.86–4.76 (m, 1H), 3.90 (br s, 3H), 3.60–3.22 (m, 6H), 1.96–1.86 (m, 4H); HRMS (ESI): *m/z* calcd for $C_{22}H_{26}N_6O_2$ $[M+1]^+$ 407.2195, found 407.2188. **14** ^{1}H NMR (400 MHz, DMSO-d_6) δ 8.48–8.41 (m, 1H), 7.36–7.26 (m, 2H), 7.04–6.90 (m, 5H), 3.90 (s, 3H), 3.82 (d, 2H, J = 6.1 Hz), 3.58–3.34 (m, 4H), 1.91 (br s, 4H); HRMS (ESI): *m/z* calcd for $C_{16}H_{21}N_7O_2$ $[M+1]^+$ 344.1835, found 344.1838. **15** ^{1}H NMR (400 MHz, DMSO-d_6) δ 8.50–8.47 (m, 1H), 7.31–7.21 (m, 1H), 7.02–6.94 (m, 4H), 4.41 (br s, 1H), 3.90 (br s, 3H), 3.54–3.24 (m, 8H), 1.90 (s, 4H), 1.62–1.44 (m, 4H); HRMS (ESI): *m/z* calcd for $C_{18}H_{26}N_6O_2$ $[M+1]^+$ 359.2195, found 359.2192. **16** ^{1}H NMR (400 MHz, DMSO-d_6) δ 8.45–8.30 (m, 1H), 7.44–7.36 (m, 2H), 7.05–6.89 (m, 3H), 4.01–3.96 (m, 2H), 3.89 (s, 3H), 3.66 (s, 3H), 3.54–3.36 (m, 4H), 1.94–1.86 (m, 4H); HRMS (ESI): *m/z* calcd for $C_{17}H_{22}N_6O_3$ $[M+1]^+$ 359.1832, found 359.1838. **17** ^{1}H NMR (400 MHz, DMSO-d_6)δ 8.46 (s, 1H), 7.54–7.43 (m, 1H), 7.16–6.94 (m, 3H), 4.70 (br s, 1H),

3.89 (s, 3H), 3.71–3.35 (m, 12H); HRMS (ESI): *m/z* calcd for $C_{16}H_{21}ClN_6O_3$ $[M+1]^+$ 381.1442, found 381.1439. **18** ^{1}H NMR (400 MHz, DMSO-d_6) δ 8.64–8.56 (m, 1H), 7.38–7.29 (m, 1H), 7.28–6.87 (m, 3H), 4.76–4.64 (m, 1H), 3.90 (s, 3H), 3.62–3.30 (m, 8H), 1.24–1.06 (m, 6H); HRMS (ESI): *m/z* calcd for $C_{16}H_{23}ClN_6O_2$ $[M+1]^+$ 367.1649, found 367.1647. **19** ^{1}H NMR (400 MHz, DMSO-d_6) δ 8.50 (d, 1H, J = 2.3 Hz),7.45–7.34 (m, 1H), 7.08–6.94 (m, 3H), 4.72–4.64 (m, 1H), 3.90 (s, 3H), 3.78–3.68 (m, 4H), 3.57–3.52 (m, 2H), 3.40–3.32 (m, 2H), 1.70–1.46 (m, 6H); HRMS (ESI): *m/z* calcd for $C_{17}H_{23}ClN_6O_2$ $[M+1]^+$ 379.1649, found 379.1659. **20** ^{1}H NMR (400 MHz, DMSO-d_6) δ 8.62–8.56 (m, 1H), 7.38–7.28 (m, 1H), 7.06–6.86 (m, 3H), 4.72–4.64 (m, 1H), 3.91 (s, 3H), 3.71–3.28 (m, 8H), 1.81–1.68 (m, 4H), 1.58–1.46 (m, 4H); HRMS (ESI): *m/z* calcd for $C_{18}H_{25}ClN_6O_2$ $[M+1]^+$ 393.1806, found 393.1805. **21** ^{1}H NMR (400 MHz, DMSO-d_6) δ 8.45–8.43 (m, 1H), 7.40–6.62 (m, 6H), 4.72 (br s, 1H), 3.89 (s, 3H), 3.53–3.26 (m, 6H), 1.58–1.48 (m, 2H), 1.40–1.30 (m, 2H), 0.93 (t, 3H, J = 7.2 Hz); HRMS (ESI): *m/z* calcd for $C_{16}H_{24}N_6O_2$ $[M+1]^+$ 333.2039, found 333.2046. **22** ^{1}H NMR (400 MHz, DMSO-d_6) δ 8.45–8.20 (m, 1H), 7.64–7.20 (m, 7H), 7.06–6.74 (m, 4H), 4.80–4.64 (m, 1H), 4.51 (d, 2H, J = 6.3 Hz), 3.87 (br s, 3H), 3.56–3.30 (m, 4H); HRMS (ESI): *m/z* calcd for $C_{19}H_{22}N_6O_2$ $[M+1]^+$ 367.1882, found 367.1889. **23** ^{1}H NMR (400 MHz, DMSO-d_6) δ 8.40–8.32 (m, 1H), 7.50–7.40 (m, 1H), 7.06–6.90 (m, 4H), 4.74–4.66 (m, 1H), 3.96–3.86 (m, 4H), 3.76–3.68 (m, 2H), 3.56–3.34 (m, 5H), 2.55–2.45 (m, 2H); HRMS (ESI): *m/z* calcd for $C_{16}H_{20}F_2N_6O_2$ $[M+1]^+$ 367.1694, found 367.1695. **24** ^{1}H NMR (400 MHz, DMSO-d_6) δ 8.42–8.38 (m, 1H), 7.41–7.33 (m, 1H), 7.04–6.93 (m, 4H), 4.79–4.64 (m, 1H), 4.09–3.98 (m, 4H), 3.89 (s, 3H), 3.56–3.50 (m, 2H), 3.40–3.32 (m, 2H), 2.34–2.40 (m, 2H); HRMS (ESI): *m/z* calcd for $C_{15}H_{20}N_6O_2$ $[M+1]^+$ 317.1726, found 317.1723. **25** ^{1}H NMR (400 MHz, DMSO-d_6) δ 8.10–7.94 (m, 1H), 7.70–7.50 (m, 1H), 7.20–7.13 (m, 2H), 7.04–6.96 (m, 1H), 6.64–6.48 (m, 1H), 4.78–4.56 (m, 1H), 3.58–3.24 (m, 8H), 2.25 (s, 3H), 1.87 (br s, 4H); HRMS (ESI): *m/z* calcd for $C_{16}H_{22}N_6O$ $[M+1]^+$ 315.1933, found 315.1938. **26** ^{1}H NMR (400 MHz, DMSO-d_6) δ 8.90–7.70 (m, 1H), 7.77–7.54 (m, 2H), 7.12 (t, 1H, J = 7.6 Hz), 6.75–6.60 (m, 2H), 4.78–4.67 (m, 1H), 3.58–3.34 (m, 8H), 2.29 (s, 3H), 1.91 (br s, 4H); HRMS (ESI): *m/z* calcd for $C_{16}H_{22}N_6O$ $[M+1]^+$ 315.1933, found 315.1940. **27** ^{1}H NMR (400 MHz, DMSO-d_6) δ 8.90–8.72 (m, 1H), 7.71 (d, 2H, J = 8.6 Hz), 7.06 (d, 2H, J = 8.0 Hz), 6.66 (br s, 1H), 4.82–4.60 (m, 1H), 3.58–3.28 (m, 8H), 2.26 (s, 3H), 1.90 (br s, 4H); HRMS (ESI): *m/z* calcd for $C_{16}H_{22}N_6O$ $[M+1]^+$ 315.1933, found 315.1938. **28** ^{1}H NMR (400 MHz, DMSO-d_6) δ 8.26–8.18 (m, 1H), 7.84–7.70 (m, 1H), 7.47 (dd, 1H, J = 8.0, 1.6 Hz), 7.32 (t, 1H, J = 7.2 Hz), 7.10–7.05 (m, 1H), 6.84–6.78 (m, 1H), 4.74–4.66 (m, 1H), 3.53–3.31 (m, 8H), 1.89 (br s, 4H); HRMS (ESI): *m/z* calcd for $C_{15}H_{19}ClN_6O$ $[M+1]^+$ 335.1387, found 335.1396. **29** ^{1}H NMR (400 MHz, DMSO-d_6) δ 9.23–9.11 (m, 1H), 8.16–8.10 (m, 1H), 7.71–7.69 (m, 1H), 7.26 (t, 1H, J = 7.8 Hz), 6.95 (d, 1H, J = 7.2 Hz), 6.83–6.77 (m, 1H), 4.75–4.65 (m, 1H), 3.58–3.36 (m, 8H), 1.92 (br s, 4H); HRMS (ESI): *m/z* calcd for $C_{15}H_{19}ClN_6O$ $[M+1]^+$ 335.1387, found 335.1391. **30** ^{1}H NMR (400 MHz, DMSO-d_6) δ 9.15–9.04 (m, 1H), 7.86 (d, 2H, J = 8.8 Hz), 7.29 (br s, 2H), 6.76 (br s, 1H), 4.76–4.67 (m, 1H), 3.56–3.32 (m, 8H), 1.91 (br s, 4H); HRMS (ESI): *m/z* calcd for $C_{15}H_{19}ClN_6O$ $[M+1]^+$ 335.1387, found 335.1391. **31** ^{1}H NMR (400 MHz, DMSO-d_6) δ 8.48–8.46 (m, 1H), 7.34–7.26 (m, 1H), 7.04–6.82 (m, 4H), 4.74–4.68 (m, 1H), 3.90 (s, 3H), 3.51–3.32 (m, 8H), 1.92 (br s, 4H); HRMS (ESI): *m/z* calcd for $C_{16}H_{22}N_6O_2$ $[M+1]^+$ 331.1882, found 331.1883. **32** ^{1}H NMR (400 MHz, DMSO-d_6) δ 8.97–8.85 (m, 1H), 7.77–7.69 (m, 1H), 7.36–7.20 (m, 1H), 7.13 (t, 1H, J = 8.2 Hz), 6.73–6.66 (m, 1H), 6.50 (dd, 1H, J = 7.6, 1.8 Hz), 4.77–4.66 (m, 1H), 3.76 (s, 3H), 3.71–3.32 (m, 8H), 1.91 (br s, 4H); HRMS (ESI): *m/z* calcd for $C_{16}H_{22}N_6O_2$ $[M+1]^+$ 331.1882, found 331.1879. **33** ^{1}H NMR (400 MHz, DMSO-d_6) δ 8.81–8.70 (m, 1H), 7.51 (d, 2H, J = 8.2 Hz), 6.85 (d, 2H, J = 8.8 Hz), 6.62 (br s, 1H), 4.77–4.66 (m, 1H), 3.74 (s, 3H), 3.69–3.32 (m, 8H), 1.90 (br s, 4H); HRMS (ESI): *m/z* calcd for $C_{16}H_{22}N_6O_2$ $[M+1]^+$ 331.1882, found 331.1888. **34** ^{1}H NMR (400 MHz, DMSO-d_6) δ 10.68 (br s, 1H), 8.16–8.12 (m, 1H), 7.83–7.75 (m, 1H), 6.93–6.76 (m, 4H), 4.74–4.68 (m, 1H), 3.56–3.37 (m, 11H), 1.91 (br s, 4H); HRMS (ESI): *m/z* calcd for $C_{15}H_{20}N_6O_2[M+1]^+$317.1726, found 317.1729. **35** ^{1}H NMR (400 MHz, DMSO-d_6) δ 8.50 (br s, 1H), 7.32–7.24 (m, 1H), 7.01–6.81 (m, 4H), 4.72 (br s, 1H), 4.20–4.13 (m, 2H), 3.56–3.34 (m, 8H), 1.91 (br s, 4H), 1.42 (t, 3H, J = 7.8 Hz); HRMS (ESI): *m/z* calcd for $C_{17}H_{24}N_6O_2$ $[M+1]^+$ 345.2039, found 345.2046. **36** ^{1}H NMR (400 MHz, DMSO-d_6) δ 8.49 (d, 1H, J = 8.0 Hz), 7.54–7.36 (m, 3H), 7.19–7.14 (m, 2H), 7.10–6.98 (m, 3H), 6.94–6.86 (m, 1H), 6.82 (t, 1H, J = 5.7 Hz), 4.74–4.60 (m, 1H), 3.56–3.31 (m, 8H), 1.92–1.86 (m, 4H); HRMS (ESI): *m/z* calcd for $C_{21}H_{24}N_6O_2$ $[M+1]^+$ 393.2039, found 393.2033. **37** ^{1}H NMR (400 MHz, DMSO-d_6) δ 8.57–8.49 (m, 1H), 7.34–7.25 (m, 1H), 7.12–7.03 (m, 2H), 6.93–6.84 (m, 2H), 4.76–4.64 (m, 1H), 3.57–3.34 (m, 8H), 1.91 (br s, 4H), 1.39 (s, 9H); ^{13}C NMR (400 MHz, DMSO-d_6, 60 °C) δ 165.5, 163.2, 163.1, 143.3, 133.8, 122.8, 121.3, 120.6, 119.3, 79.6, 60.0, 45.4, 42.8, 28.4, 28.4, 24.4. HRMS (ESI): *m/z* calcd for $C_{19}H_{28}N_6O_2$ $[M+1]^+$ 373.2352, found 373.2356. **38** ^{1}H NMR (400 MHz, DMSO-d_6) δ 8.47 (br s, 1H), 7.54–7.29 (m, 7H), 7.12–6.93 (m, 2H), 6.86–6.81 (m, 1H), 5.23–5.21 (m, 2H), 4.71–4.66 (m, 1H), 3.60–3.32 (m, 8H), 1.90 (br s, 4H); HRMS (ESI): *m/z* calcd for $C_{22}H_{26}N_6O_2$ $[M+1]^+$ 407.2195, found 407.2202. **39** ^{1}H NMR (400 MHz, DMSO-d_6) δ 8.20 (d, 1H, J = 8.0 Hz), 8.10–7.96 (m, 1H), 7.38–7.33 (m, 2H), 7.18–7.13 (m, 1H), 6.77–6.75 (m, 1H), 4.72–4.63 (m, 1H), 3.48–3.33 (m, 8H), 1.89 (br s, 4H); HRMS (ESI): *m/z* calcd for $C_{16}H_{19}F_3N_6O_2$ $[M+1]^+$ 385.1600, found 385.1602. **40** ^{1}H NMR (400 MHz, DMSO-d_6) δ 8.12–8.07 (m, 1H), 7.88–7.83 (m, 1H), 7.49–7.40 (m, 1H), 7.25 (t, 1H, J = 7.4 Hz), 7.10–7.08 (m, 1H), 6.79 (t, 1H, J = 5.7 Hz), 4.72–4.65 (m, 1H), 3.52–3.30 (m, 8H), 2.42 (s, 3H), 1.90 (br s, 4H); HRMS (ESI): *m/z* calcd for $C_{16}H_{22}N_6OS$ $[M+1]^+$ 347.1654, found 347.1659. **41** ^{1}H NMR (400 MHz, DMSO-d_6) δ 8.25–8.10 (m, 1H), 7.21–7.16 (m, 1H), 6.75–6.60 (m, 2H), 6.51 (br s, 1H), 4.78–4.64 (m, 1H), 3.86 (s, 3H), 3.75 (s, 3H), 3.57–3.26 (m, 8H), 1.94–1.84 (m, 4H); HRMS (ESI): *m/z* calcd for $C_{17}H_{24}N_6O_3$ $[M+1]^+$ 361.1988, found 361.1987. **42** ^{1}H NMR (400 MHz, DMSO-d_6) δ 8.30–8.24 (m, 1H), 7.30–7.21 (m, 1H), 6.96–6.84 (m 2H), 6.50 (dd, 1H, J = 8.8, 2.9 Hz), 4.78–4.64 (m, 1H), 3.86 (s, 3H), 3.77 (s, 3H), 3.56–3.24 (m, 8H), 1.90 (br s, 4H); HRMS (ESI): *m/z* calcd for $C_{17}H_{24}N_6O_3$ $[M+1]^+$ 361.1988, found 361.1991. **43** ^{1}H NMR (400 MHz, DMSO-d_6) δ 9.01–8.95 (m, 1H), 7.47–7.39 (m, 1H), 7.33 (d, 1H, J = 8.4 Hz), 7.21 (d, 1H, J = 8.4 Hz), 7.00–6.86 (m, 1H), 4.73–4.63 (m, 1H), 3.99 (s, 3H), 3.54–3.26 (m, 8H), 1.92 (br s, 4H); HRMS (ESI): *m/z* calcd for $C_{17}H_{21}F_3N_6O_2$ $[M+1]^+$ 399.1756, found 399.1760. **44** ^{1}H NMR (400 MHz, DMSO-d_6) δ 8.99–8.87 (m, 1H), 7.66 (d, 2H, J = 7.4 Hz), 7.48–7.26 (m, 5H), 7.12 (d, 1H, J = 8.4 Hz), 6.88–6.83 (m, 1H), 4.60–4.49 (m, 1H), 3.95 (s, 3H), 3.60–3.40 (m, 8H), 1.92 (br s, 4H); HRMS (ESI): *m/z* calcd for $C_{22}H_{26}N_6O_2$ $[M+1]^+$ 407.2195, found 407.2192. **45** ^{1}H NMR (400 MHz,

DMSO-d_6) δ 9.58 (d, 1H, J = 7.2 Hz), 8.51–8.26 (m, 1H), 8.07 (t, 1H, J = 8.6 Hz), 7.72–7.67 (m, 1H), 7.22–7.17 (m, 1H), 6.93–6.87 (m, 1H), 4.78–4.65 (m, 1H), 3.58–3.28 (m, 8H), 1.89 (br s, 4H); HRMS (ESI): m/z calcd for $C_{15}H_{19}N_7O_3$ $[M+1]^+$ 346.1628, found 346.1622. **46** ^{1}H NMR (400 MHz, DMSO-d_6) δ 10.86–10.82 (m, 1H), 8.91–8.83 (m, 1H), 8.18 (s, 1H), 7.74 (dd, 1H, J = 8.0, 1.6 Hz), 7.60 (s, 1H), 7.48–7.44 (m, 1H), 7.00–6.82 (m, 2H), 4.72–4.70 (m, 1H), 3.57–3.33 (m, 8H), 1.91 (br s, 4H); HRMS (ESI): m/z calcd for $C_{16}H_{21}N_7O_2$ $[M+1]^+$ 344.1835, found 344.1839. **47** ^{1}H NMR (400 MHz, DMSO-d_6) δ 9.78–9.70 (m, 1H), 8.13–8.01 (m, 1H), 7.85 (s, 1H), 7.43 (d, 1H, J = 7.6 Hz), 7.17–7.03 (m, 2H), 6.82–6.77 (m, 1H), 4.71–4.65 (m, 1H), 3.51–3.33 (m, 8H), 2.10 (s, 3H), 1.89 (br s, 4H); HRMS (ESI): m/z calcd for $C_{17}H_{23}N_7O_2$ $[M+1]^+$ 358.1991, found 358.1994. **48** ^{1}H NMR (400 MHz, DMSO-d_6) δ 10.83 (br s, 1H), 8.19–8.09 (m, 1H), 7.90 (br s, 1H), 7.04–6.83 (m, 3H), 4.82–4.60 (m, 1H), 3.61–3.24 (m, 8H), 1.92 (br s, 4H); HRMS (ESI): m/z calcd for $C_{15}H_{19}ClN_6O_2$ $[M+1]^+$ 351.1336, found 351.1334. **49** ^{1}H NMR (400 MHz, DMSO-d_6) δ 10.74 (br, 1H), 8.34–8.15 (m, 2H), 7.63–7.60 (m, 2H), 7.45 (t, 2H,J = 7.6), 7.32 (t, 1H, J = 7.2 Hz), 7.24–7.20 (m, 1H), 6.96–6.94 (m, 2H), 4.71 (br s, 1H), 3.57–3.30 (m, 8H), 1.92 (br s, 4H); HRMS (ESI): m/z calcd for $C_{21}H_{24}N_6O_2$ $[M+1]^+$ 393.2039, found 393.2050. **50** ^{1}H NMR (400 MHz, DMSO-d_6) δ 8.67 (s, 1H), 7.34–7.26 (m, 1H), 7.06–6.93 (m, 3H), 4.74–4.64 (m, 1H), 4.20–4.12 (m, 2H), 3.58–3.31 (m, 8H), 1.93 (br s, 4H), 1.42 (t, 3H, J = 7.0 Hz); HRMS (ESI): m/z calcd for $C_{17}H_{23}ClN_6O_2$ $[M+1]^+$ 379.1649, found 379.1648. **51** ^{1}H NMR (400 MHz, DMSO-d_6) δ 8.69 (d, 1H, J = 2.3 Hz), 7.31–7.23 (m, 1H), 7.07–6.90 (m, 3H), 4.72–4.67 (m, 2H), 3.57–3.34 (m, 8H), 1.93 (br s, 4H), 1.34 (d, 6H, J = 5.3 Hz); HRMS (ESI): m/z calcd for $C_{18}H_{25}ClN_6O_2$ $[M+1]^+$ 393.1806, found 393.1815. **52** ^{1}H NMR (400 MHz, DMSO-d_6) δ 8.69 (s, 1H), 7.34–7.25 (m, 1H), 7.12 (d, 1H, J = 8.6 Hz), 7.04–6.92 (m, 2H), 4.73–4.67 (m, 1H), 3.57–3.31 (m, 8H), 1.93 (br s, 4H), 1.40 (s, 9H); HRMS (ESI): m/z calcd for $C_{19}H_{27}ClN_6O_2$ $[M+1]^+$ 407.1962, found 407.1966. **53** ^{1}H NMR (400 MHz, DMSO-d_6) δ 8.97–8.86 (m, 1H), 7.85 (d, 2H, J = 8.6 Hz), 7.25 (t, 2H, J = 7.8 Hz), 6.92 (t, 1H, J = 7.4 Hz), 6.69 (br s, 1H), 4.76–4.66 (m, 1H), 3.57–3.31 (m, 8H), 1.91 (br s, 4H); HRMS (ESI): m/z calcd for $C_{15}H_{20}N_6O$ $[M+1]^+$ 301.1777, found 301.1774.

18. *GC enzyme assay*. Assays were conducted using recombinant GC (Cerezyme®, Genzyme Co., Cambridge, MA) and resorufin-β-D-glucopyranoside (K_m = 28 μM) in an assay buffer composed of 50 mM citric acid/KH_2PO_4, pH 5.9, 10 mM sodium taurocholate and 0.01% Tween 20. GC in assay buffer was added to a 1536-well black plate at 2 μl/well, followed by addition of 23 nl of compound in DMSO with a pin-tool station (Kalypsys, San Diego). After 5 min at RT (~21 °C), 1 μl/well of substrate was added and incubated for 20 min at RT. Fluorescence intensity was measured at an excitation of 570 (±10) nm and an emission of 610 (±10) nm. The final concentrations of enzyme and substrate were 1.9 nM and 30 μM, respectively. *Enzyme selectivity assays.* Three additional hydrolases and their substrates, α-glucosidase (from rice) and 4-methylumbelliferyl α-D-glucopyranoside (4MU-α-Glc), α-galactosidase (from coffee beans) and 4-methylumbelliferyl α-D-galactopyranoside (4MU-α-Gal), and β-*N*-acetylglucosaminidase (from bovine kidney) (HEX) and 4-methylumbelliferyl *N*-acetyl-β-D-glucosaminide (4MU-β-GSM) were obtained from Sigma–Aldrich. The buffer for all three enzyme assays consisted of 50 mM citric acid/KH_2PO_4, pH 4.5, 10 mM sodium taurocholate and 0.01% Tween 20. The final enzyme concentrations for α-glucosidase, α-galactosidase and β-*N*-acetylglucosaminidase were 8, 1 and 8 nM, respectively. The substrate concentrations were similar to the K_m values for these related enzymes, at 0.4, 0.16 and 0.2 mM, respectively.